Quarterly Progress Report 4

Radar Studies of the Moon

15 November 1966

Prepared for the U.S. National Aeronautics and Space Administration
under Contract NSR 22-009-106 by

Lincoln Laboratory

MASSACHUSETTS INSTITUTE OF TECHNOLOGY

Lexington, Massachusetts

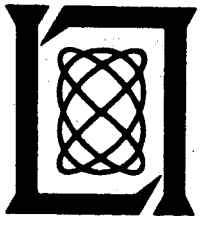

The work reported in this document was performed at Lincoln Laboratory, a center for research operated by Massachusetts Institute of Technology; this work was supported by the U.S. National Aeronautics and Space Administration under Contract NSR 22-009-106.

Quarterly Progress Report

4

Radar Studies of the Moon

15 November 1966

Issued 23 November 1966

Prepared for the U.S. National Aeronautics and Space Administration
under Contract NSR 22-009-106 by

Lincoln Laboratory

MASSACHUSETTS INSTITUTE OF TECHNOLOGY

Lexington, Massachusetts

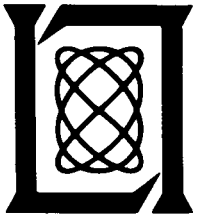

FOREWORD

This is the fourth Quarterly Progress Report under Contract NSR 22-009-106 between the National Aeronautics and Space Administration and Lincoln Laboratory, M.I.T. The first three of these reports will be referred to as QPR (1966:1), QPR (1966:2) and QPR (1966:3), respectively, in this report.

During this quarterly period, significant progress has been made in the development of instrumentation and the derivation of initial results in certain previously unreported areas. An account is given of the work which has been carried out in preparation for the radiometric studies at wavelengths of 2.0 and 3.7 cm. Also reported are the status of the high-resolution mapping program at a wavelength of 3.8 cm and the progress with the 8-mm radar system. The radiometric studies require relatively straightforward use of station instrumentation but have not been emphasized until recently. In both the high-resolution mapping and 8-mm radar studies areas, the development of the instrumentation is substantially more complicated than for the L- and X-band cross-section, scattering law and polarization measurements previously reported as largely complete.

CONTENTS

RADAR STUDIES OF THE MOON

I. THERMAL EMISSION FROM THE MOON AT 2.0 AND 3.7 CM

Since the subject of thermal emission from the moon has not been discussed in previous quarterly progress reports, we shall very briefly review the theory of this emission and particularly attempt to clarify the types of physical parameters which are related to it. Some previous radiometric work carried out elsewhere will then be reviewed and compared with the current experimental program. The procedure for taking the radiometric data and for analyzing such data is explained and some results, together with their preliminary interpretation, are given.

A. Lunar Brightness Temperature at Microwave Frequencies

It has been shown repeatedly that at microwave frequencies in excess of 1 MHz, radiation reflected from the lunar surface due to sources of radiation such as the sun is completely negligible compared with the thermal emission from the moon (Davies and Gardner, 1966; Moran, 1965). Hence, we shall be concerned with only the true thermal emission from the lunar surface.

The brightness temperature has been computed on the basis of simple models of the lunar surface material by Piddington and Minnet (1949), and by Troitsky (1954) whose model involves a plane interface between vacuum and a homogeneous slightly lossy dielectric layer. This assumption should be adequate if the surface irregularities are small and if the depth of origin of the thermally emitted waves is negligible compared with the radius of curvature of the surface. Troitsky's calculation assumes that the actual lunar surface temperature is a known function of time and of position on the moon. The boundary value of the temperature is used to compute the heat conduction and hence the temperatures at points below the surface. From the known temperatures, the amount of thermal emission and therefore the surface brightness temperature is computed by standard methods. This brightness temperature must be related to antenna temperature through parameters describing the performance of the antenna and receiver system.

The surface temperature T_S (i.e., at depth $z = 0$) is given by

$$T_S(\varphi, \Theta, t) = \sum_{n=0}^{\infty} T_n(\Theta) \cos [n\Omega t - n\varphi - \epsilon_n(0)] \quad . \tag{1}$$

Here, φ and Θ are lunar longitude and latitude coordinates, respectively, $\Omega = 2\pi/P$ where P is the synodic period of the moon, and where it is assumed that the lunar surface is laterally homogeneous so that longitude variations in $T_n(\Theta)$ and $\epsilon_n(\Theta)$ vanish, and that there are no thermal

sources inside the moon. Under these assumptions (according to Troitsky, 1954), the brightness temperature T_B of a point on the lunar surface should be given by

$$T_B(\varphi, \Theta, t) = (1 - R^2) \left\{ T_o(\Theta) + \sum_{n=1}^{\infty} \frac{T_n(\Theta) \cos [n\Omega t - n\varphi - \epsilon_n(\Theta) - \gamma_n]}{\sqrt{1 + 2\delta_n \cos r' + 2\delta_n^2 \cos^2 r'}} \right\} \tag{2}$$

where

r' = angle inside medium between surface normal and ray arriving at observer

$$\delta_n = \beta_n / k_\nu$$

$$\beta_n = \sqrt{\frac{n\Omega\rho S}{2K}} = \beta_1 \sqrt{n} \tag{3}$$

ρ, S, k = density, specific heat and thermal conductivity

k_ν = power attenuation coefficient for electromagnetic wave of observation

$$\gamma_n = \tan^{-1} \frac{\delta_n \cos r'}{1 + \delta_n \cos r'} \quad . \tag{4}$$

The quantity R^2 describes the amount of reflection at the interface and is a function of the angle r' and of the polarization of the electromagnetic radiation. For a simple interface between vacuum and a plane dielectric medium, R^2 is identical with the square of the Fresnel reflection coefficients. When the simple interface is not plane, as is certainly the case for the lunar surface, or when the interface has a double layer structure, the reflection coefficient is somewhat more complex as will be discussed in greater detail below.

Provided the surface temperature is adequately known, a study of the microwave emission from a given point on the moon as a function of time will directly give a value for δ_n which basically measures the ratio of depth of penetration of an electromagnetic wave at the frequency of observation to the depth of penetration of the thermal variations.

The problem of knowing the surface temperature is apparently a difficult one. The surface temperature ideally should be determined at infrared frequencies by observations. However, this appears to be difficult since few observational results are available; also, this is indicated by the fact that quite large discrepancies exist between the temperatures quoted by different observers, particularly in regard to lunar night temperatures. For the subsolar point, a value of 400°K seems to be in reasonable agreement with observations (Pettit and Nicholson, 1930; Moroz, 1966). For the nighttime value, different observers quote values from 120° to 100°K (Pettit and Nicholson, 1930; Murray and Wildey, 1964; Shorthill and Saari, 1965). Theoretically, the surface temperature should arise from a solution of the heat conduction equation

$$\frac{\partial T}{\partial t} = \frac{k}{\rho \cdot S} \cdot \frac{\partial^2 T}{\partial z^2} \tag{5}$$

with the boundary condition

$$(1 - R_i)\, \sigma T_S^4 - (1 - R_c)\, S_o f(t) = k \cdot \left(\frac{\partial T}{\partial z}\right)_{z=0} \tag{6}$$

where S_o is the solar constant, R_i is a mean reflectivity at infrared wavelengths, σ is the constant of proportionality in Stefan Boltzmann's Law, R_c is a mean reflectivity at optical wavelengths and f(t) is the time variation of the insolation. Solution of these equations with a value of $(k\rho S)^{-1/2} = 1000$ seems to indicate a longitude dependence of the temperature of approximately $\cos^{1/4}\varphi$, whereas observations actually appear to be more in agreement with $\cos^{1/6}\varphi$, a discrepancy attributed to surface roughness (Troitsky, 1965).

Hence, one may state briefly that a study of the variation of the lunar brightness temperature with lunar phase provides a direct measure of the ratio of penetration of thermal waves and electromagnetic waves, and that the accuracy of the determined ratio depends on the accuracy with which the surface temperature is known.

B. Linear Polarization of Emission

Because of the factor $(1 - R^2)$ in Eq. (2) above, the emitted radiation will be polarized linearly, in the direction of the local plane of incidence. The degree of polarization is determined by the ratio of the transmission coefficients for radiation polarized in and across the local plane of incidence. For a completely smooth plane surface of slightly lossy dielectric material, this ratio is determined by the ratio of the transmission coefficients, since the thermal radiation inside the lossy dielectric is unpolarized. The polarization p of the radiation emitted at an angle of incidence r is given by

$$\frac{P_{||} - P_{\perp}}{P_{||} + P_{\perp}}$$

where

$P_{||}$ = power emitted with polarization in plane of incidence,

$P_{\perp}$ = power emitted with polarization normal to plane of incidence, and the ratio

$$\frac{P_{||}}{P_{\perp}} = \frac{\epsilon\left(\cos r + \sqrt{\epsilon - \sin^2 r}\right)^2}{\left(\epsilon \cos r + \sqrt{\epsilon - \sin^2 r}\right)^2} \quad .$$

The polarization p is plotted in Fig. 1 as a function of angle r, with ϵ (the dielectric constant) as a parameter.

The polarization or power ratio actually observed will be smaller than this for several reasons. Because the beamwidth of the antenna is finite, the power in the two orthogonally polarized receiver channels will correspond to an averaging over a certain angular interval so that the curves shown in Fig. 1 will represent only a limiting case for infinitely narrow beamwidths. The effect of the polar diagram smoothing has been subjected to preliminary studies by convolving one-dimensional Gaussian polar diagrams of varying half-widths with a distribution of emission corresponding to a constant disk temperature for several values of the dielectric constant ϵ. An example of the polarization resulting from this convolution is shown in Fig. 2, where the apparent polarization is plotted against the position of the center of the beam for $\epsilon = 2.0$ for several different antenna beamwidths. The effect of antenna beam convolution for other than uniform temperature distributions will be studied in detail in a future report.

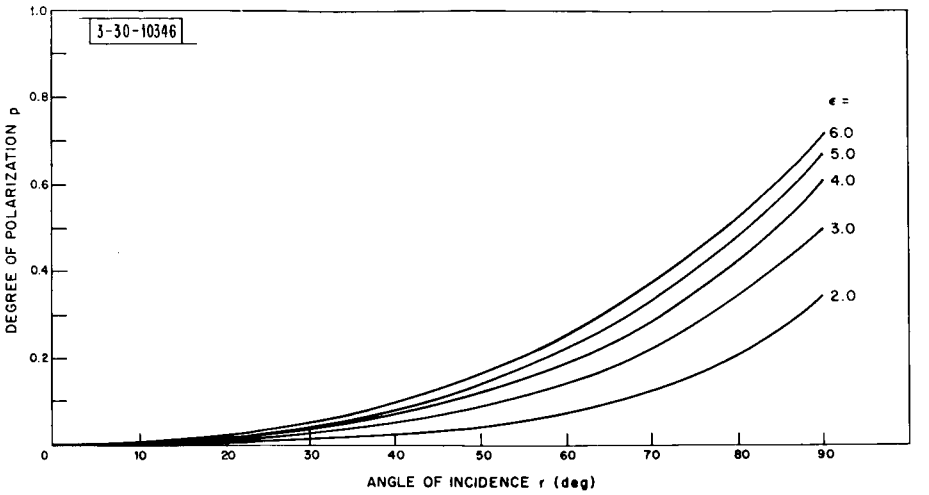

Fig. 1. Degree of polarization p vs angle of incidence r for simple homogeneous dielectric model. Parameter ϵ.

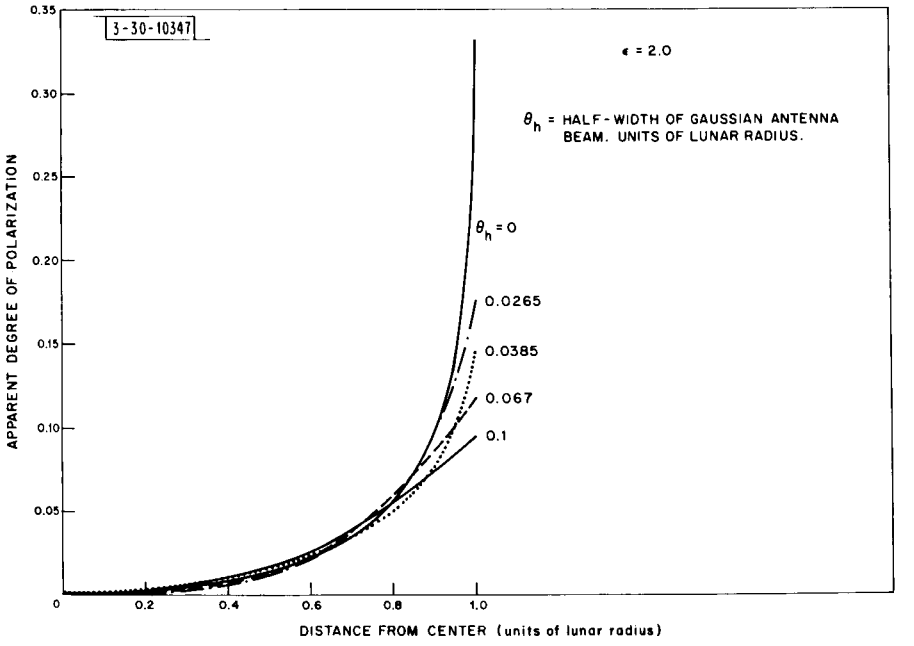

Fig. 2. Apparent degree of polarization observed with antenna of finite beamwidth – emission from ideal dielectric and smooth surface.

The observed polarization may also be reduced by the presence of surface undulations whose effect is to smear the power distribution over the disk over a certain range of angles corresponding to the tilts of the surface with respect to the mean surface. Irregularity effects have been studied in some detail by Hagfors and Morriello (1965). The change in the degree of polarization for various models of the surface irregularities is shown in Figs. 3(a) through (c). In Fig. 3(a), the surface undulations are described by a Gaussian autocorrelation function

$$\rho(\Delta r) = \exp[-\Delta r^2/2L^2]$$

and the parameter S is defined as the ratio of h_o and L, h_o being the rms height deviation of the surface from a mean surface. In Fig. 3(b), the surface is described by an exponential autocorrelation function of the form

$$\rho(\Delta r) = \exp[-\Delta r/\ell]$$

and the parameter C is defined by

$$C^2 = \ell^2/(h_o^4 k^2 \sqrt{\epsilon - 1})$$

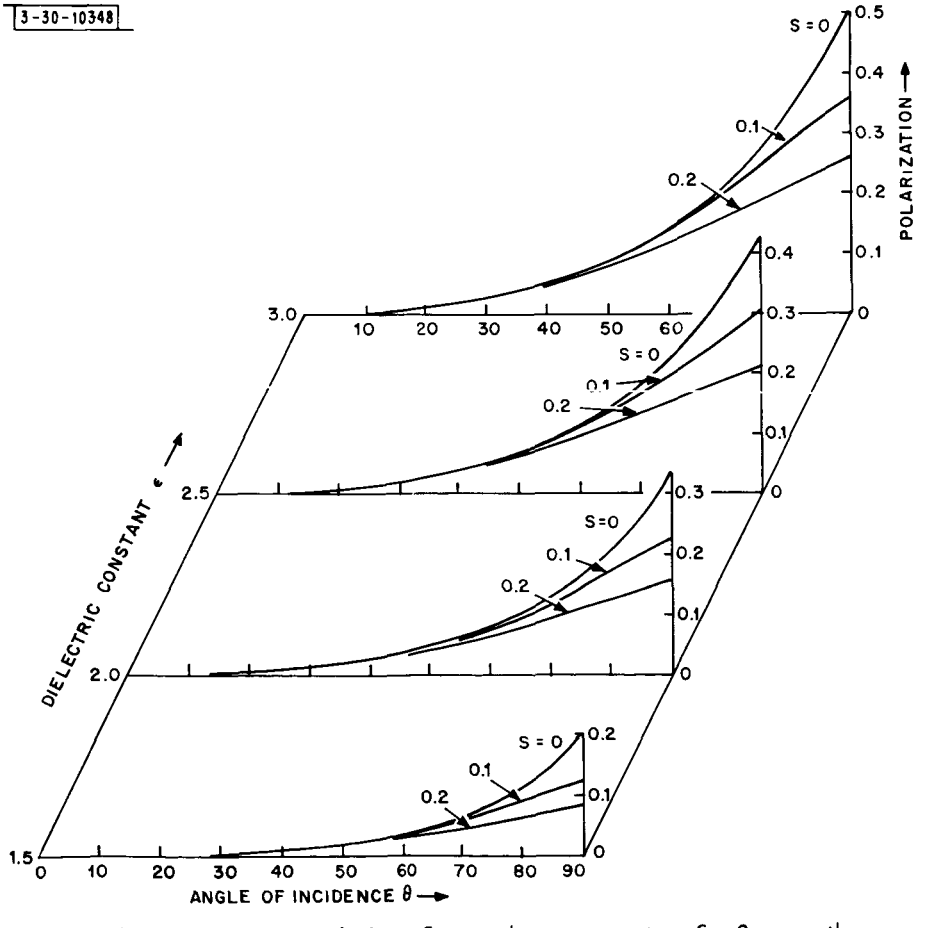

(a) Gaussian autocorrelation: S = roughness parameter; S = 0 = smooth.

Fig. 3(a-c). Polarization of thermal emission from dielectric surface for various types of random surfaces.

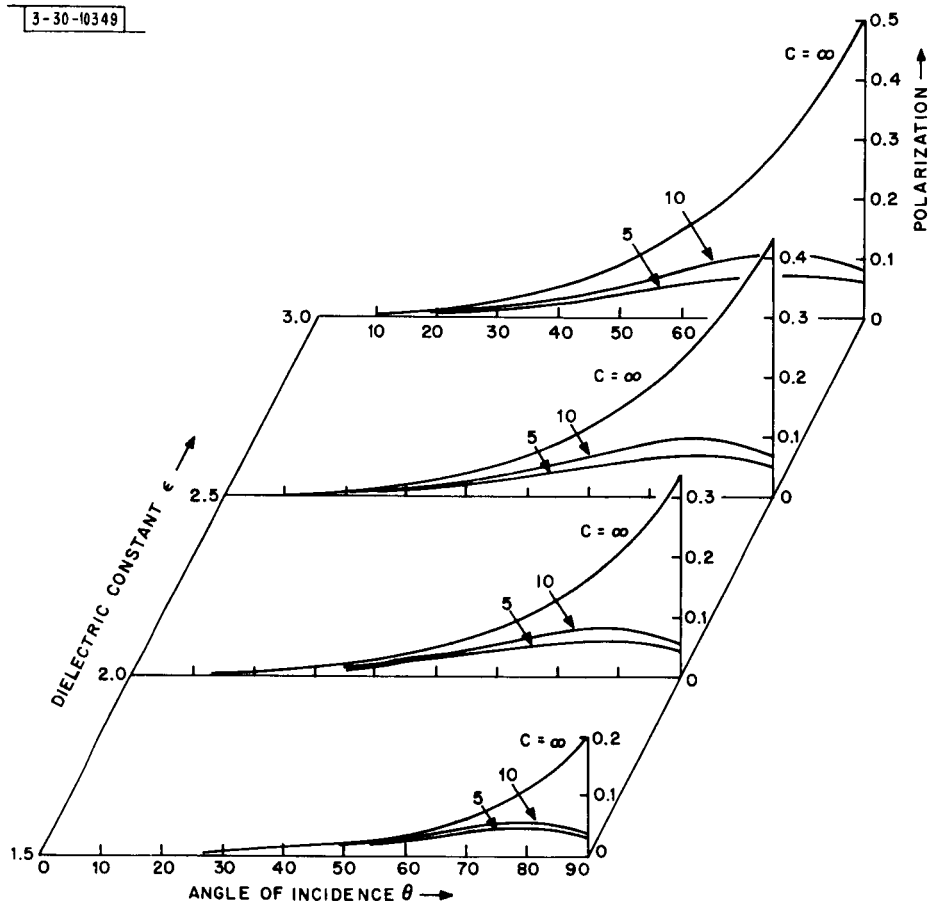

(b) Exponential autocorrelation: C = roughness parameter; C = ∞ = smooth.

Fig. 3. Continued.

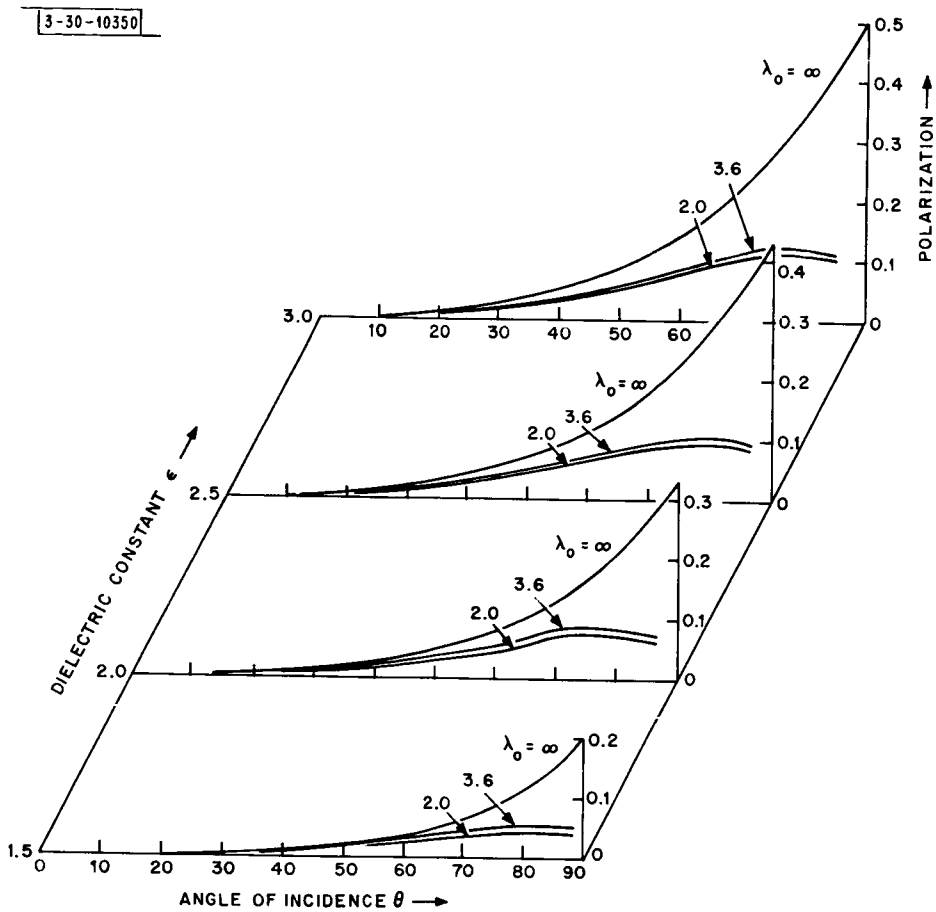

(c) Surface roughness derived from lunar radar data.

Fig. 3. Continued.

with $k = 2\pi/\lambda$. For Fig. 3(c), the surface irregularities were derived from radar data as presented by Evans and Pettengill (1963). These calculations will be discussed in greater detail in a future report.

Finally, there may be a modification of the degree of polarization as shown in Fig. 3 if the transition from vacuum to the medium is not sudden but involves a more-or-less gradual transition. The case of a homogeneous, thick double layer of random depth has been treated. In this case, the ratio $P_{||}/P_{\perp}$ can be shown to be given by

$$\frac{P_{||}}{P_{\perp}} = \frac{\epsilon_2\left(\cos r + \sqrt{\epsilon_2 - \sin^2 r}\right)\left[\cos r\sqrt{\epsilon_2 - \sin^2 r} + (\epsilon_1 - \sin^2 r)\right]}{\left(\epsilon_2 \cos r + \sqrt{\epsilon_2 - \sin^2 r}\right)\left[\epsilon_1 \cos r\sqrt{\epsilon_2 - \sin^2 r} + \frac{\epsilon_2}{\epsilon_1}(\epsilon_1 - \sin^2 r)\right]}$$

where ϵ_1 is the dielectric constant of the transition layer, and ϵ_2 is that for the supporting layer. Figure 4 shows the degree of polarization vs angle of incidence r for a supporting layer with $\epsilon_2 = 5.0$ for different values of ϵ_1. It is interesting to observe that for near-grazing incidence the degree of polarization is primarily determined by the properties of the upper layer.

Other cases of transition layers, such as one involving a linear gradient in dielectric constant with depth, which has been considered in connection with radar reflection near normal incidence (Hagfors, 1966), cannot easily be discussed because of difficulties in solving the wave equation for both polarizations. However, it does seem that the direct comparison between radiometric and radar observations may serve to make the possible surface models less ambiguous than if radar observation results only were available.

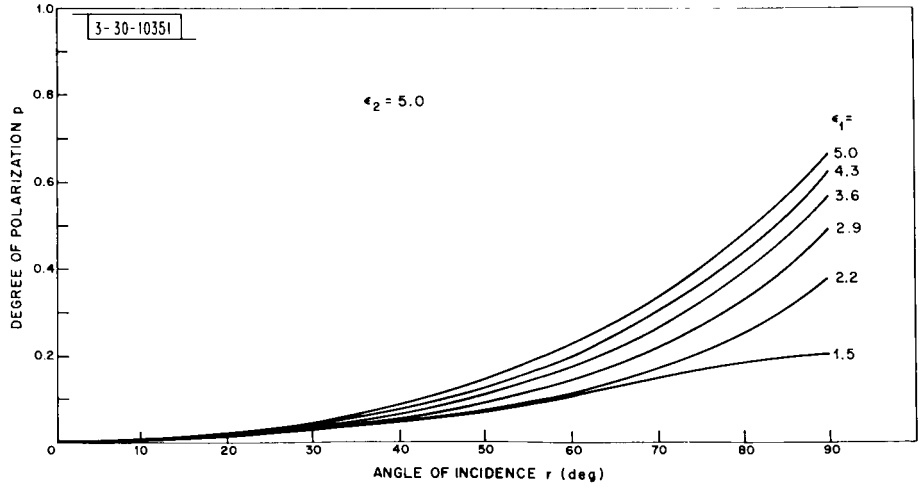

Fig. 4. Polarization of thermal emission from double-layer model, thick homogeneous top layer of random depth supported by layer with $\epsilon_2 = 5.0$.

C. Observational Procedure and Preliminary Results

Radiometric observations have been made of the moon at 3.7 cm using the Haystack antenna and the regular radiometer system used for general radio astronomy use. The equipment consists of two radiometer channels, each of 500-MHz bandwidth, adjacent to each other in frequency. With a receiver system temperature of about 1200°K and an integration time per data point of 2 sec, the statistical uncertainty in the temperature determination is less than 0.1°K.

The feed system is linearly polarized and the linear primary feed system can be rotated physically by remote control from the operator's console. The setting of the linear dipole is accurate to 1.8°, which was considered adequate for the experiment. The half-power beamwidth of the antenna is approximately 0.07° or about 4.5 minutes of arc. The sidelobes are down by more than 20 db.

Because of the azimuth-altitude mount of the Haystack antenna system, the direction of the linearly polarized dipole primary feed will normally be oriented with respect to the horizon system. For reasons of convenient comparison of data obtained at different times, the primary feed of the antenna was oriented with respect to the direction of the lunar axis for these measurements. Each observation consists of a complete set of drift scans with the linearly polarized feed aligned with the projection of the lunar axis, and another set of scans with the feed perpendicular to this axis. The drift scans were repeated with declination offsets from the center of the moon stepped by 0.035° between scans. The polarization was adjusted between scans for appropriate alignment with the selenographic coordinate system. No adjustments were made during individual scans.

The antenna temperature integrated over 2 sec was recorded every 2 sec on magnetic tape, on a line printer and on a regular pen chart recorder. The baseline was derived by fitting a straight line to the noise data at the beginning and end of each drift scan. In order to smooth the data contained in the individual drift scans after the baseline correction, the data were expanded into a Fourier series and a certain amount of truncation of this series was applied. It was found that expansion to 25 terms was adequate, and this is now generally used. Examples of two such smoothed drift scans are shown in Fig. 5(a-b). Scan (a) was obtained with the linearly polarized feed approximately aligned with the direction of scan, whereas scan (b) was obtained with the feed approximately normal to the direction of the scan. The excess of emission when the linearly polarized feed is approximately aligned with the local plane of incidence is clearly visible.

The two smoothed sets of drift scans are normalized to 100° at the center of the moon for each of the two polarizations, and contour maps are constructed of normalized antenna temperature for both polarizations as well as for the difference of the two temperatures. Examples of such contour maps are shown in Fig. 6(a-b), where (a) is obtained with feed normal to lunar axis and (b) with feed along lunar axis. The contours, which at present unfortunately are still unlabeled, correspond to the sequence of normalized temperatures: 50, 70, 90, 92, 94, 96, 98, 100 and 102°. Also shown in Fig. 6 is an illustration of the illuminated part of the moon at the time of observation. The relation between the microwave emission and the illumination of the lunar surface is clearly visible.

In Fig. 7, a contour diagram of the difference in antenna temperatures is shown for the data of Fig. 6. The temperature difference contours are 2° apart. Preliminary analysis of the data on the basis of a smooth one-layer moon appears to give a dielectric constant of 1.7 to 1.8.

-30-10352

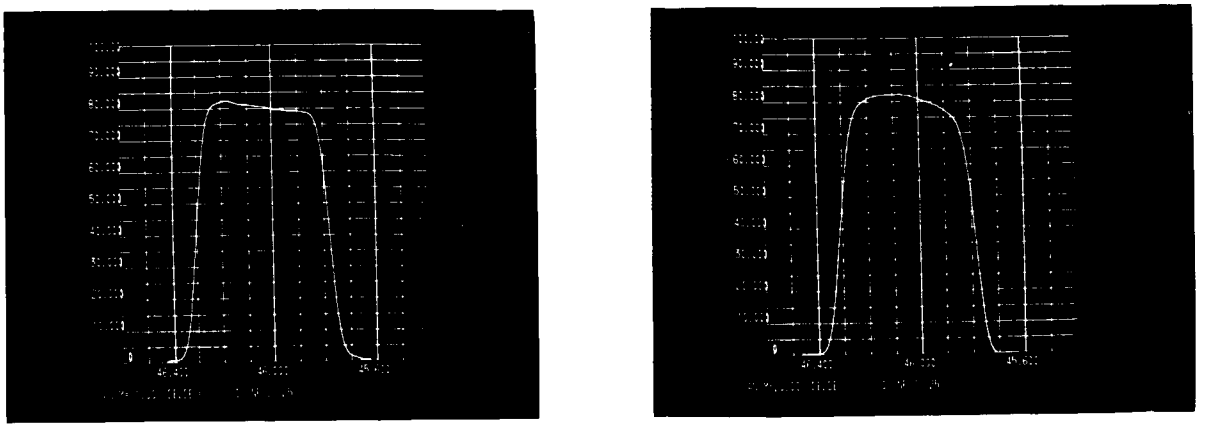

(a) (b)

WAVELENGTH 3.7 cm

Fig. 5. Smoothed drift scans, through center of lunar disk. (a) Feed aligned approximately with direction of scan; (b) feed approximately normal to direction of scan (data obtained 13 July 1966).

-30-10353

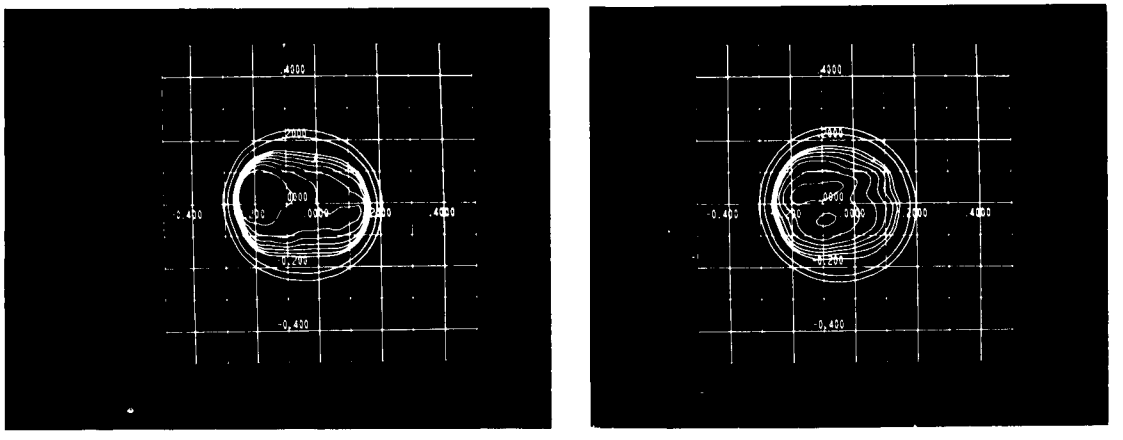

(a) (b)

WAVELENGTH 3.7 cm

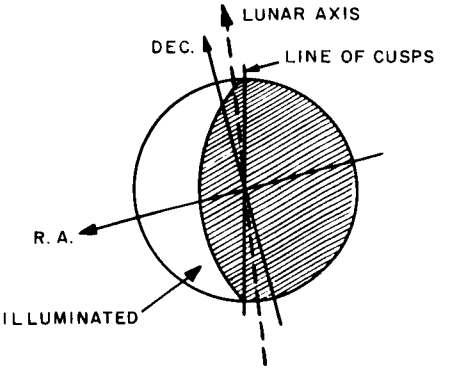

Fig. 6. Contour plots of normalized emission temperature for two polarizations: (a) feed normal to lunar axis, (b) feed aligned with lunar axis (data obtained 13 July 1966).

At present, six apparently successful runs are available for analysis, and they will be analyzed as computer time is available. We plan to extend the measurements at 3.7 cm to include a full lunation and to conduct a similar set of observations at 2.0 cm by early 1967.

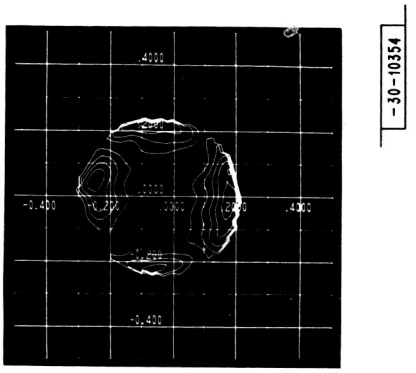

Fig. 7. Difference of two contour plots shown in Fig. 6.

II. HIGH-RESOLUTION 3.8-CM REFLECTIVITY MAPPING

During the current reporting period, work has centered primarily on increasing the input ephemeris accuracy and in exploring and improving the method of output mapping display. Major changes in the Haystack transmitting and receiving systems required for other research being conducted at the station have prevented the accumulation of more raw radar data during this quarterly period. However, the backlog of data stored during July 1966 has proven sufficient to support continued development of the processing and presentation methods and to provide some preliminary results. The improvements in overall system sensitivity and reliability should greatly enhance the quality of the data to be taken during the remainder of the program.

A. Ephemeris Improvements

As pointed out previously [QPR (1966:3), p. 23], a slight discrepancy has been noted between the measured and predicted values for the delay and Doppler shift of the nearest portion of the moon. The slowly varying part of this discrepancy is presumably related to small errors in the lunar ephemeris. While of considerable interest in developing a deeper understanding of the moon's motions, these errors do not interfere with the mapping program since they may be determined by direct radar measurement every several hours and allowed for in the intervening mapping runs. What has been troublesome is a more rapidly varying component in the Doppler discrepancy which changes sufficiently over several hours to make the correction of the mapping data difficult – at least to the desired accuracy of 0.1 Hz.

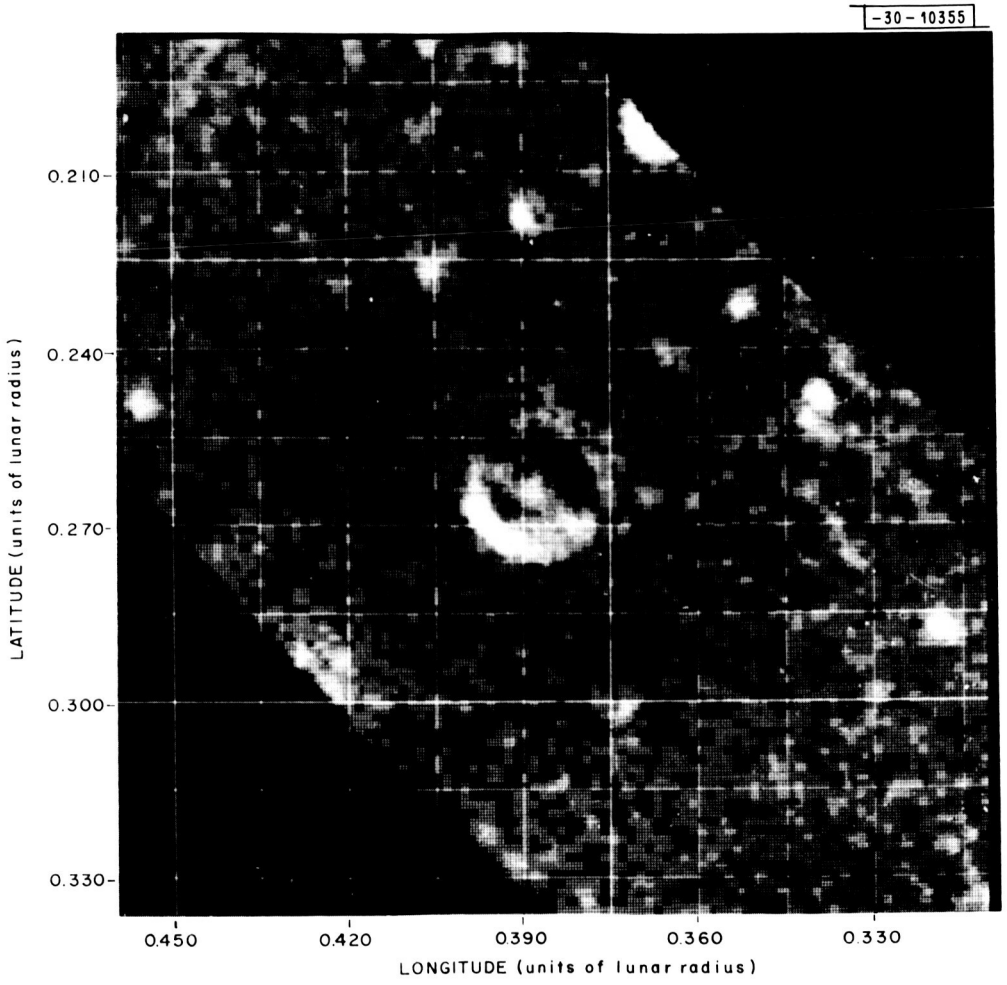

Fig. 8. Computer-generated display of 3.8-cm radar-reflectivity map of region surrounding Plinius on lunar surface. Mapping resolution is roughly 2×2 km as represented by patchwork square. Data taken by Haystack radar on 20 July 1966.

The rapidly varying component of Doppler error has now been traced to truncation of the hourly values of horizontal parallax supplied by the Naval Observatory. In an attempt to improve and stabilize the estimates in the rate of change of horizontal parallax, values extending over 5 days (for a total of 121 values of parallax) are converted to a radius vector from earth and fitted with an ellipse having three degrees of freedom: semimajor axis, eccentricity and in-plane orientation (argument of perihelion). Following the fit, the improved values of radius corresponding in angular location to the original data points are derived from the best-fit ellipse and converted back to parallax. From these stabilized values of parallax, the Doppler is calculated as before from a power series expansion in time.

While inelegant from a theoretical point of view, this approach seems likely to provide the desired stabilization with least effort and in a manner quite compatible with the existing programs. It does not require the very intensive effort that would accompany a full attack on the basic lunar orbital motion, although this is anticipated by another group in Lincoln Laboratory in the near future.

B. Preliminary Results of High-Resolution 3.8-cm Mapping

Considerable effort has been expended during the current reporting period on improving the method of presenting the data obtained from the mapping program. These maps, like a television picture, contain an immense detail of information in numerical form. Two approaches have been followed through to completion: the first permits extremely high resolution – up to 300 × 300 positional cells in latitude and longitude, each one having any one of 64 levels of intensity; the second uses a series of ten distinct dot patterns to represent ten levels of intensity. Their larger size limits a given computer display to 100 × 100 positional resolution elements, but removes the photographic film response from the calibration requirements, since the dot pattern for each level is quite recognizable. The first method of display permits a "quick-look" over a considerable area; the second permits a quantitative analysis of a more restricted region.

A preliminary result using the first method is shown in Fig. 8, and covers the same region as shown in Figs. 17 through 20 of QPR (1966:3). For comparison, Fig. 19 of that report is reproduced here as Fig. 9. The resolution in Fig. 8 is limited to 100 × 100 cells by the radar mapping; the individual cells may be seen as squares in the display and correspond to areas roughly 2 × 2 km on the lunar surface. The semicircular boundaries at upper right and lower left arise from the limitations in the number of range gates sampled in the original data taking.

Note the remarkable resemblance between the major craters in the radar and optical photographs. The portions of the crater walls whose normals tilt toward the radar are brighter, while those that tilt away are darker, yielding an appearance of shadowing. The low-level fluctuation arises from the measurement statistics (this is only a 5-min. run) and will be reduced in the 20-min. "production" runs. An example of the second display approach was not available in time for inclusion in this report.

III. PROGRESS IN 8-MM RADAR SYSTEM

The chief activity in the 8-mm section of the program has been preparation for the conversion of the radar to dual polarization. New equipment nearing completion for this purpose includes an RF head, a two-channel receiver and a two-polarization transmitter for the antenna test range. Two attempts to detect the moon with interim system configurations failed as a result of equipment problems.

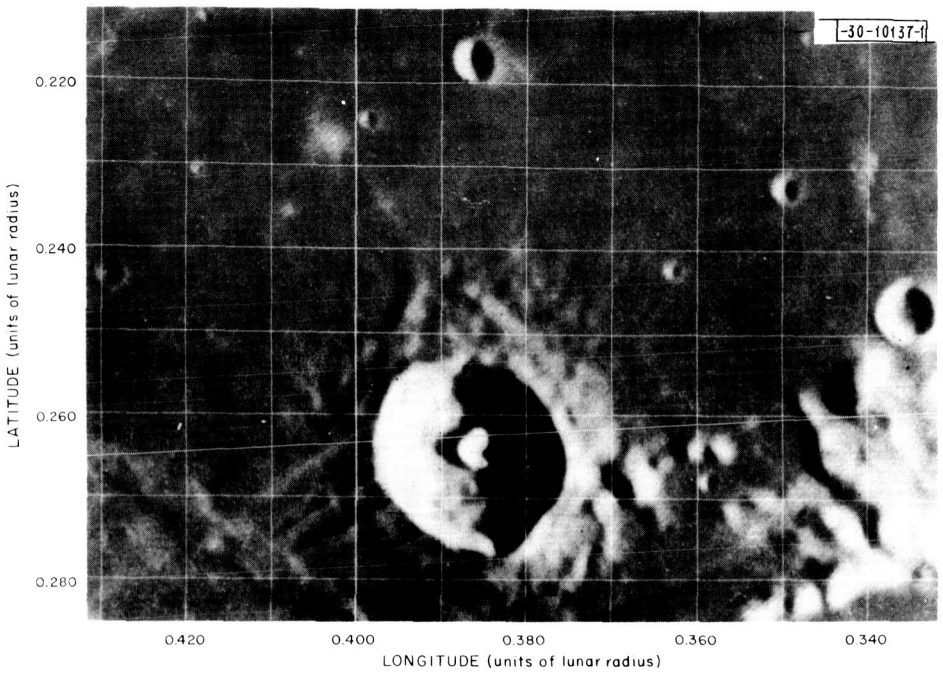

Fig. 9. Telescopic photograph of region of lunar surface in vicinity of Plinius (University of Chicago Lunar Atlas). Compare with radar data given in Fig. 8.

A. System Development

The RF head includes a 50-watt Elliott 8FK15 klystron and a solid-state multiplier that converts 5 MHz to 35 GHz for stabilizing the klystron by phase locking (so that the receiver can have a bandwidth of 100 Hz or less) and for supplying local-oscillator power to the receiver. It also includes an orthogonal-mode transducer, an adjustable phase shifter and a quarter-wave retarder. The last three items are waveguide components for controlling the polarization of the transmitted and received radiation. The polarization can be circular or in any selected plane, and the receiver channels respond either to right- and left-hand circular, or to two orthogonal-plane polarizations. Waveguide switches enable the operator to choose the received polarization independently of the transmitted polarization, except that if both are plane, one receiver channel is in the same plane as the transmitted wave.

A less flexible RF head would be quicker to build and would have somewhat less loss in waveguide, but all the complexity has to be present if one is to transmit circular polarization and receive two orthogonal-plane polarizations. This is a vital mode of operation for some of the more interesting measurements, e.g., the evaluation of the scattering coefficients for radiation polarized in and normal to the plane of incidence. The complexity of the RF head can therefore not be reduced without postponing an experiment that should have high priority.

The orthogonal-mode transducer and the quarter-wave retarder have been electroformed in our shop. Tests have shown that the transducer is free of unwanted modes; testing of its impedance characteristics is under way.

The two-channel receiver has successive intermediate frequencies of 30 MHz, 2.215 MHz and 2.500 kHz. Each low-frequency channel incorporates a comb filter with five channels 170 Hz

wide, spaced 100 Hz apart. The circuits are the same as in the present single-channel receiver, except that there are fewer channels in the comb filter. A frequency synthesizer acting as the second local oscillator is programmed, by means of punched tape, to convert the received frequency to a constant 2.215 MHz in spite of the changing Doppler shift caused by relative motion of moon and earth. If this compensation for Doppler shift is programmed correctly for the area on which the beam impinges, all the received signal passes through the central filter of the comb; the function of the other filters is to reveal small errors in the Doppler-compensating program and to aid in improvising changes in the synthesizer settings when one wishes to look at an area on the moon for which the Doppler shift has not been computed.

The test range for the antenna uses a low-power klystron transmitter mounted on a 100-ft water tower 6 miles from the radar. The installation presently transmits horizontal polarization; the conversion to dual polarization demands more elaborate equipment. A new 4-ft dish capable of transmitting horizontal or vertical polarization is nearly ready to be erected on the tower, and a 4-inch square horn capable of receiving these polarizations is being calibrated prior to installation on the edge of the radar antenna, where it will serve as a standard against which the gain of the radar antenna will be measured.

In the 1963 version of the radar, the antenna feed was a circular waveguide leading from the cab to a point very near the focus, together with a flat mirror directly in front of the open end of the waveguide. The pipe was 0.351 inch in diameter and 14 ft long with a one-way loss of 1.4 db. Recently, a waveguide 0.480 inch in diameter has been installed in the hope of reducing the feedline loss. There were doubts that the larger guide would be usable because, in order to provide proper illumination of the dish, the orifice that irradiates the flat mirror has to retain the 0.351-inch diameter; thus, the larger pipe can support modes that cannot escape through the hole at the end, and it seemed possible that trapping of the unwanted modes would cause large losses at resonances so closely spaced as to render the feed useless for radar work. Extensive experiments have shown, however, that the transmission dips caused by the resonances of unwanted modes amount to only about 0.2 db. In these experiments, the round pipe was fed through a normal rectangular waveguide and an electroformed transition. It is expected that feeding the pipe by means of an orthogonal-mode transducer and polarizer will not seriously raise the level of excitation of the unwanted modes, and that the old waveguide run can be replaced by the larger one, which at 35 GHz has a one-way loss of only 0.75 db. The resulting reduction in two-way loss is 1.3 db.

Work on the 1000-watt transmitter is continuing at a slow rate, which will accelerate as the delivery of the kilowatt tube nears. The vendor has made an experimental tube that ran at 750 watts for 1 hour. The gain of this 5-cavity tube was 33 db. Since we require 47 db, a sixth cavity will be added and an improvement in the output coupling will be sought. Except perhaps for the gain, the difficult problems seem to be under control; a deliverable tube will probably be available by 15 January 1967, the scheduled date.

A visit to the supplier showed that the multiplier design for the kilowatt transmitter is progressing well. Though some problems are yet to be solved, this vendor expects to meet the scheduled delivery date of 15 November 1966.

B. Operations

On 24 August 1966, there was an attempt to detect an echo from the moon using horizontal polarization and a 10-watt transmitter. When it failed, most of the parts of the radar were tested

individually in an effort to determine the cause of the experiment's failure. The transmitted power, antenna gain and receiver sensitivity were all at about the levels used when Lynn, et al. (1963) successfully detected the moon. To see whether the boresight telescope-television combination might become misaligned when the dish was elevated above the position used for boresighting on the test range, the antenna was pointed at the sun. Passive detection of the sun at 35 GHz showed both the boresighting and the receiver sensitivity to be good. This test seemed to show also that the antenna feed line is unobstructed, since the signal-to-noise ratio obtained on the sun was the same as that observed in 1963. A spectral purity test could not be performed at this time because the multiplier that normally provides a 35.030-GHz reference wave that is beat against the transmitter had been sent back to the factory for repair. Lacking any other explanation of failure to see the moon, we suspected that the multiplier in the phase-lock system was putting out a poor spectrum, so that too much of the energy in the echo failed to pass through the narrow passband of the receiver.

As soon as the multiplier was repaired, a new attempt was made to see the moon. This aborted because an amplidyne in the antenna drive burned out. The ensuing shutdown provided a good opportunity to install one of the recently received 50-watt tubes. However, it proved impossible to phase-lock this tube for more than a few seconds at a time. The faults seem to lie not in the tube itself, but in its power and control circuits. Corona caused by the higher voltages required for this tube was one problem. Another was an oscillation at about 2 MHz in the phase-locking modulator, caused by the inductance of one of the protective relays. This has been eliminated.

The tube arced sporadically, and the protective circuits appear to have operated too slowly, because eventually the tube refused to function. The power supplies and associated circuits have now been moved to the laboratory, where they will be improved before operation of the second 50-watt tube is attempted. The radar is again operating with the 10-watt tube, and a new attempt to see the moon at this level will be made as soon as weather permits.

ACKNOWLEDGMENTS

The work of most of the technical personnel of Group 31, Surveillance Techniques, which operates the facilities of the Field Station, in preparing and conducting the work reported to date is gratefully acknowledged, as is the work of members of Group 46, Microwave Components, in cooperating with Dr. McCue on the 8.6-mm radar.

The use of the facilities of the Lincoln Laboratory Millstone-Haystack complex, provided by the U. S. Air Force, is also gratefully acknowledged.

REFERENCES

Davies, R.D., and Gardner, F.F., "Linear Polarization of the Moon at 6, 11 and 21 cm Wavelength," to be published.

Evans, J.V., and Pettengill, G.H., "The Scattering Behavior of the Moon at Wavelengths of 3.6, 68, and 784 Centimeters," J. Geophys. Res. 68, 423-447 (1963).

Hagfors, T., "A Study of the Depolarization of Lunar Radar Echoes," NEREM Conference, Boston, 2-4 November 1966.

Hagfors, T., and Morriello, J., "The Effect of Roughness on the Polarization of Thermal Emission from a Surface," J. Res. Natl. Bur. Stds., Radio Science 69D, 1614-1615 (1965).

Lynn, V.L., Sohigian, M.D., and Crocker, E.A., "Radar Observations of the Moon at 8.6-mm Wavelength," Technical Report 331, Lincoln Laboratory, M.I.T. (8 October 1963), DDC 426207; see also J. Geophys. Res. 69, 781 (1964).

Moran, J.M., "Radiometric Observations of the Moon Near 1 cm Wavelength," S.M. Thesis, Department of Electrical Engineering, M.I.T. (June 1965).

Moroz, V.I., "Infrared Spectrophotometry of the Moon and the Galilean Satellites of Jupiter," Soviet Astronomy 9, 999 (1966).

Murray, B.C., and Wildey, R.L., "Surface Temperature Variations During the Lunar Nighttime," Astrophys. J. 139, 734 (1964).

Pettit, E., and Nicholson, S.B., "Lunar Radiation and Temperatures," Astrophys. J. 71, 102 (1930).

Piddington, J.H., and Minnet, H.C., "Microwave Thermal Radiation from the Moon," Australian J. Sci. Res. 2A, 63 (1949).

Shorthill, R.W., and Saari, J.M., "Radiometric and Photometric Mapping of the Moon through a Lunation," Annals of the New York Academy of Sciences 123, Art. 2, 722-739 (15 July 1965).

Troitsky, V.S., "On the Theory of Lunar Radio Emission," Astron. Zh. 31, 511 (1954).

_____, "Investigation of the Surfaces of the Moon and Planets by the Thermal Radiation," J. Res. Natl. Bur. Stds., Radio Science 69D, 1585-1612 (1965).